

Supporting information

**Sulfate-reducing bacteria (SRB) can enhance the uptake of  
silver-containing nanoparticles in a wetland plant**

Zuo-shun Niu<sup>a</sup>, Yi Yang<sup>abc\*</sup>, Fei-yun Tou<sup>a</sup>, Xing-pan Guo<sup>ad</sup>, Rong Huang<sup>e</sup>, Jie Xu<sup>f</sup>, Yu-ru Chen<sup>a</sup>,  
Li-jun Hou<sup>b</sup>, Min Liu<sup>ad</sup>, Michael F. Hochella, Jr.<sup>gh</sup>

<sup>a</sup> Key Laboratory of Geographic Information Science of the Ministry of Education, School of Geographic Sciences, East China Normal University, 500 Dongchuan Road, Shanghai 200241, China

<sup>b</sup> State Key Laboratory of Estuarine and Coastal Research; Yangtze Delta Estuarine Wetland Ecosystem Observation and Research Station, Ministry of Education & Shanghai, East China Normal University, 3663 North Zhongshan Road, Shanghai 200062, China

<sup>c</sup> Shanghai Key Lab for Urban Ecological Processes and Eco-Restoration, East China Normal University, 500 Dongchuan Road, Shanghai 200241, China

<sup>d</sup> Institute of Eco-Chongming, East China Normal University, 500 Dongchuan Road, Shanghai 200241, China

<sup>e</sup> Key Laboratory of Polar Materials and Devices, Ministry of Education, East China Normal University, Shanghai 200062, China

<sup>f</sup> Department of Geological Sciences, the University of Texas at El Paso, 500 W University Avenue, El Paso, TX 79968, USA

<sup>g</sup> Subsurface Science and Technology Group, Energy and Environment Directorate, Pacific Northwest National Laboratory, Richland, Washington 99352, United States

<sup>h</sup> NanoEarth, Department of Geosciences, Virginia Tech, Blacksburg, Virginia 24061, United States

\*Corresponding author: Yi Yang (yyang@geo.ecunu.edu.cn)

**1. Materials and methods**

**Isolation and identification of SRB.**

The sediments collected from Yangtze Estuary were added to a liquid medium (the composition of the medium is listed in Supporting Information (SI) Table S1), and the suspension was then cultured under anaerobic conditions at 25 °C until it turned black. The suspension was subsequently cultured using the dilution coating-stack sandwich culture method, and a single colony was isolated and purified. The purified bacterial strain was grown overnight in LB liquid medium under anaerobic conditions. After centrifugation at 10000 g for 10 min, the supernatant was discarded and genomic DNA was extracted using a 3S DNA Isolation Kit for Environmental Samples V 2.2 following the manufacturer's instructions (Shenergy Biocolor Bioscience and Technology Company, Shanghai, China). The 16S rRNA gene sequence of the genomic DNA was amplified by PCR using primer sets of 27 F (5' - AGAGTTTGATCCTGGCTCAG - 3') and 1492 R (5' - GGTTACCTTGTTACGACTT - 3').<sup>1</sup> The PCR amplification was performed in a 25 µL reaction mixture containing 0.5 µL of each primer (10 µM), 1 µL of template DNA, 12.5 µL of Taq PCR Master Mix (2 ×, with blue dye), and sterile distilled water to a final volume of 25 µL. Thermal cycling was conducted under the following conditions: an initial denaturing step at 94 °C for 5 min, followed by 35 cycles of denaturation at 94 °C for 30 s, annealing at 55 °C for 30 s, and elongation at 72 °C for 2 min. Finally, an extension step was performed at 72 °C for 8 min. PCR products and their sizes were verified by agarose gel electrophoresis (1.0% weight/volume agarose) with ethidium bromide staining in a 1× TAE buffer at 120 V for 15 min and visualized using an ultraviolet (UV) transilluminator. PCR products were sequenced by the Shanghai Map Biotech Company Ltd. The 16S rRNA gene sequences obtained were analyzed with the BLAST program of the GenBank database at the National Center for Biotechnology Information (NCBI) website (<http://www.ncbi.nlm.nih.gov/>).

**Table S1.** Composition of cell culture media used for the SRB isolation.

Chemicals	Content
K <sub>2</sub> HPO <sub>4</sub>	0.5 g
(NH <sub>4</sub> ) <sub>2</sub> SO <sub>4</sub>	1.0 g
MgSO <sub>4</sub>	2.0 g
L(+)-Ascorbic acid	0.5 g

L-Cysteine	0.5 g
Na <sub>2</sub> SO <sub>4</sub>	5.0 g
Sodium DL-Lactate	6.5 g
FeSO <sub>4</sub>	0.5 g
Milli-Q water	1 L

---

### **TEM characterization of 40 nm and 80 nm Ag<sup>0</sup>-NPs.**

The 40- and 80-nm Ag<sup>0</sup>-NP standard solutions were homogenized using an ultrasonic instrument. Approximately 7 µL of solution was dropped onto a TEM grid (CF300-Cu, Electron Microscopy Science), and the TEM grid was dried in a desiccator prior to TEM analysis.

## **2. Results and discussion**

### **Characterization of Ag<sup>0</sup>-NPs.**

Based on the results obtained with a TEM coupled with EDS and SAED, the measured sizes of Ag<sup>0</sup>-NPs were generally consistent with the expected sizes (20, 40 and 80 nm), as shown in Fig. S1A, B and C. The major elemental compositions of these Ag<sup>0</sup>-NPs were C, Cu and Ag, and the strong C and Cu signals obtained in the EDS analysis can be attributed to the Cu-based TEM grids. Moreover, 20-nm Ag<sup>0</sup>-NPs showed *d*-spacings of 2.38, 2.05 and 1.18 Å, corresponding to *d*-spacings of planes (1 1 1), (2 0 0) and (2 2 2), respectively, of silver.<sup>2</sup> 40 nm Ag<sup>0</sup>-NPs exhibited *d*-spacings of 2.35, 1.99 and 1.22 Å, corresponding to the (1 1 1), (2 0 0) and (3 1 1) lattice planes, respectively, of silver.<sup>3</sup> In addition, Ag<sup>0</sup>-NPs with an average size of 80 nm showed *d*-spacings of 2.40, 2.00 and 1.46 Å, which matches the (1 1 1), (2 0 0) and (2 2 0) lattice planes of silver, respectively.<sup>2</sup>

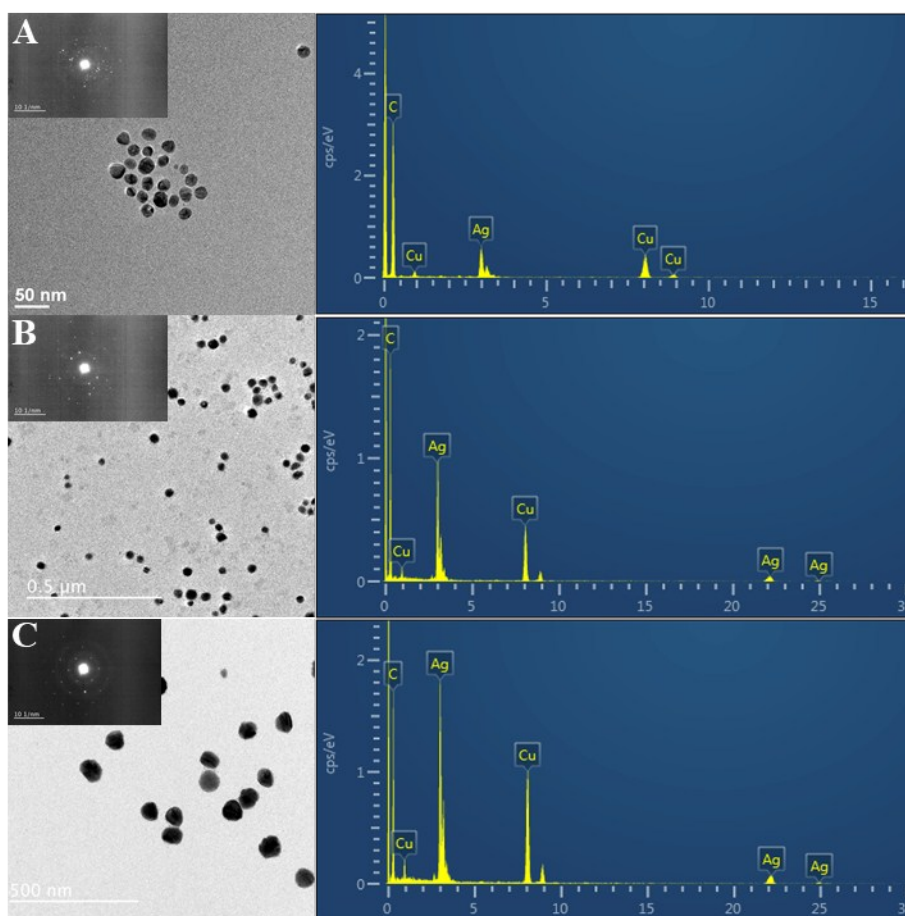


**Figure S1.** Representative TEM images, EDS and SAED analysis of Ag<sup>0</sup>-NPs with different sizes.(A: 20-nm Ag<sup>0</sup>-NPs, B: 40-nm Ag<sup>0</sup>-NPs, C: 80-nm Ag<sup>0</sup>-NPs)

**Table S2.** Zetasizer analysis of 20-nm Ag<sup>0</sup>-NPs in Hoagland solution in the presence/absence of SRB. The hydrodynamic diameters were not detected in 0.01 and 0.1 mg/L 20-nm Ag<sup>0</sup>-NPs suspension in Hoagland solution as the result of that the concentration of Ag<sup>0</sup>-NPs were too low to reach the detected concentration. “+”: in the presence of SRB; “-”: in the absence of SRB.

Ag concentration[ mg/L]	0.01		0.1		1		10	
SRB	-	+	-	+	-	+	-	+
Zeta-potential[ mV]	-5.58±0.43	-8.74±1.07	-5.39±0.60	-8.21±0.77	-6.03±1.21	-10.21±0.43	-4.82±0.09	-9.17±0.63
Hydrodynamic Diameter[ nm]	—	—	—	—	56.00±3.23	75.05±2.86	46.13±0.34	63.94±0.69

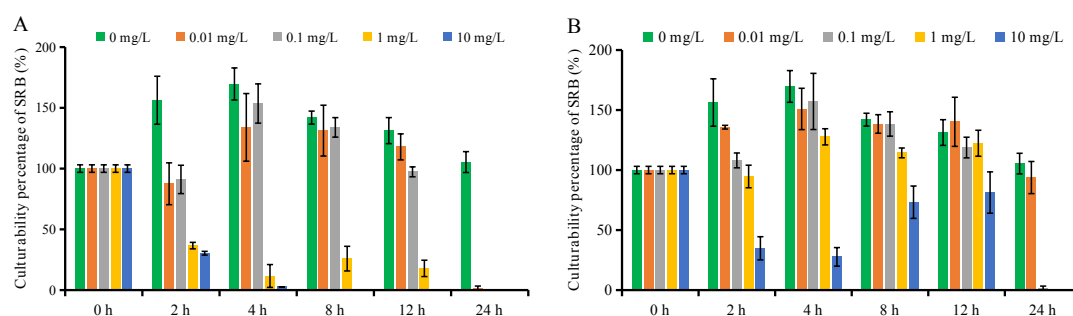


**Figure S2.** Dose and time-dependent culturability percentage of SRB in the presence of silver ions and 20 nm Ag<sup>0</sup>-NPs in Hoagland solution. A: treated with silver ions; B: treated with 20-nm Ag<sup>0</sup>-NPs

**Table S3.** Ratios (%) of total Ag concentrations in the whole plants treated with SRB versus those without SRB (i.e. R<sub>+/-</sub>) for Ag<sup>+</sup> and 20-nm Ag<sup>0</sup>-NPs treatment groups.

Concentration	Time	Ag <sup>+</sup> treatment group	20-nm Ag <sup>0</sup> -NPs treatment group
0.01	1 day	18.97	143.33
	3 day	43.73	119.38
	5 day	47.90	180.71
	7 day	79.13	203.58
0.1	1 day	47.66	138.49
	3 day	63.93	114.17
	5 day	42.46	151.99
	7 day	50.63	164.32
1	1 day	71.50	107.22
	3 day	85.20	184.00
	5 day	93.67	168.98
	7 day	89.26	131.41
10	1 day	98.10	171.00
	3 day	66.98	163.37
	5 day	59.82	103.63
	7 day	44.46	247.90
Average		62.71	155.84

Maximum		98.10	247.90
Minimum	□	18.97	103.63

---

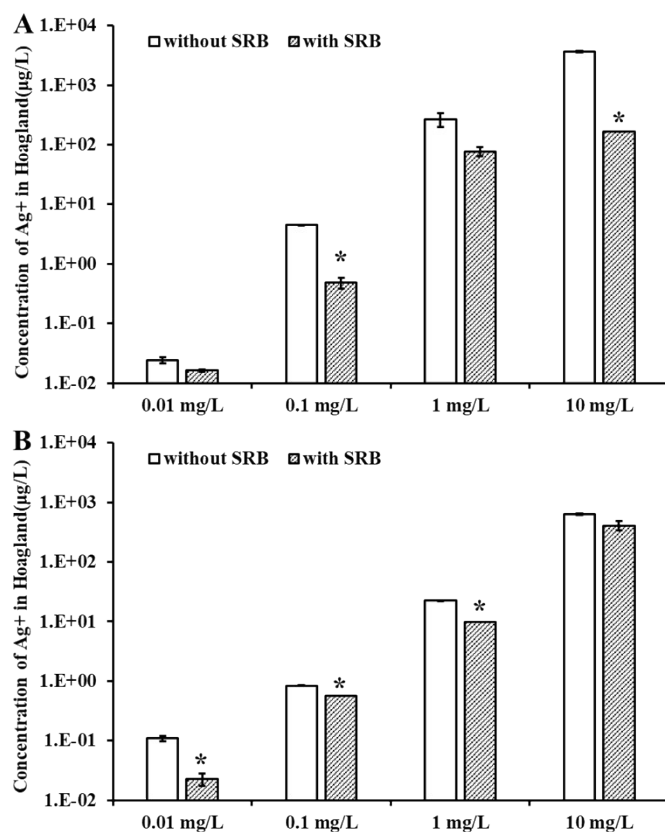


**Figure S3.** Concentrations of  $\text{Ag}^+$  in the Hoagland solution after treating plants for 1 day. A: silver ions treated Hoagland solution; B: 20 nm  $\text{Ag}^0$ -NPs treated Hoagland solution. \*: Significant difference,  $P < 0.05$ .

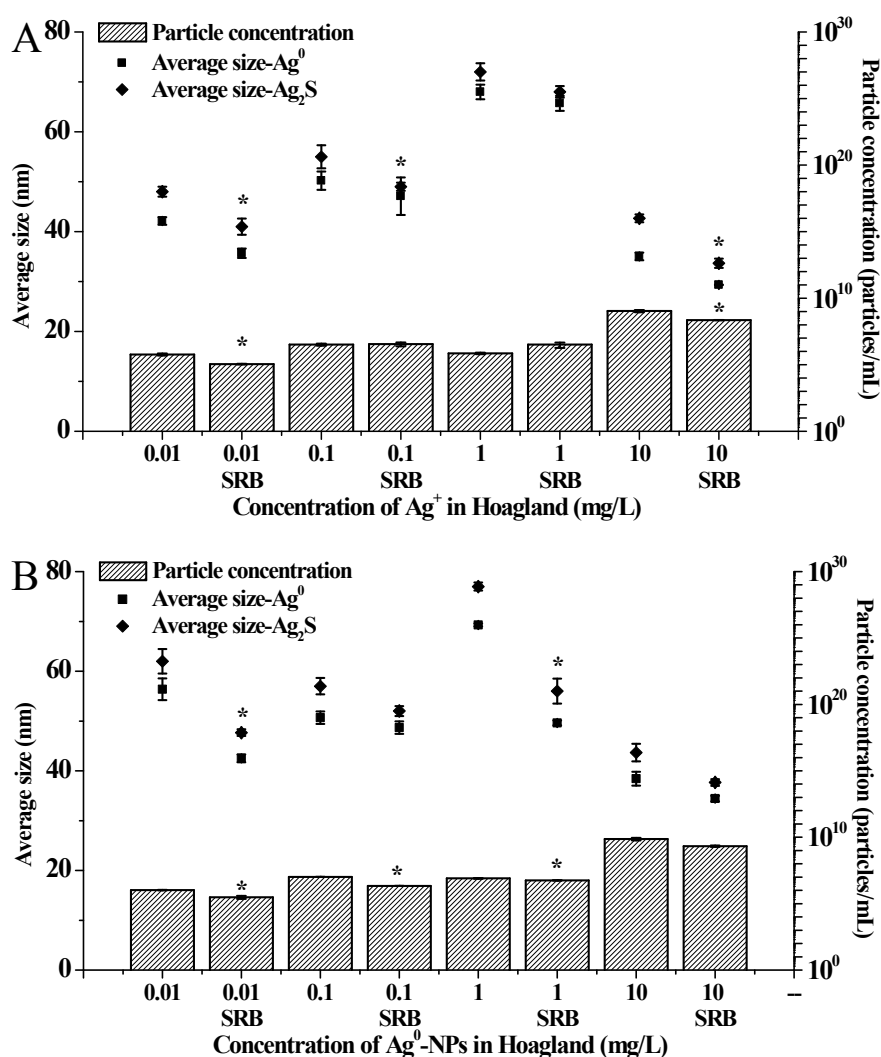


**Figure S4.** Particle concentrations and average sizes of Ag-NPs in the Hoagland solution after treating plants for 1 day. A: silver ions treated Hoagland solution; B: 20-nm  $\text{Ag}^0$ -NPs treated Hoagland solution. 0.01/0.1/1/10 SRB: Hoagland solution treated in the presence of SRB; 0.01/0.1/1/10: Hoagland solution treated in the absence of SRB. Average size- $\text{Ag}^0$ : the average sizes were calculated based on  $\text{Ag}^0$ ; Average size- $\text{Ag}_2\text{S}$ : the average sizes were calculated based on  $\text{Ag}_2\text{S}$ . \*: Significant difference,  $P < 0.05$ .

#### Characterization of Ag-NPs associated with plant roots.

Based on the results obtained with a TEM coupled with EDS and SAED data, the morphology, composition and crystal structures of the Ag-NPs associated with *Scirpus triqueter* roots were also investigated. The results provided in Fig. S5 revealed the presence of Ag-NPs of various sizes and shapes in/on plant roots after treatment with  $\text{Ag}^+$  or  $\text{Ag}^0$ -NPs in the presence/absence of SRB. For

example, a metallic silver NP was found to be associated with plant roots exposed to 20-nm  $\text{Ag}^0$ -NPs in the absence of SRB, with the silver exhibiting  $d$ -spacings of 2.35 and 1.99 Å, corresponding to the (1 1 1) and (2 0 0) lattice planes, respectively.<sup>3</sup> The plant roots exposed to 20-nm  $\text{Ag}^0$ -NPs in the presence of SRB exhibited an  $\text{Ag}_2\text{S}$ -NP aggregate with  $d$ -spacings of 3.56 and 2.58 Å, corresponding to the (0 1 1) and (0 2 2) lattice planes, respectively, of acanthite.<sup>4</sup> Moreover, we observed  $\text{Ag}_2\text{S}$ -NPs associated with plant roots exposed to 20-nm  $\text{Ag}^0$ -NPs in the absence of SRB. This result is consistent with the findings reported by Stegemeier et al., who found that both  $\text{Ag}_2\text{S}$  and  $\text{Ag}^0$ -NPs could be formed in plants hydroponically exposed to either  $\text{Ag}^+$  or  $\text{Ag}^0$ -NPs in the absence of SRB,<sup>5</sup> likely due to the reduction of sulfate by biomolecules in plants.<sup>6, 7</sup>



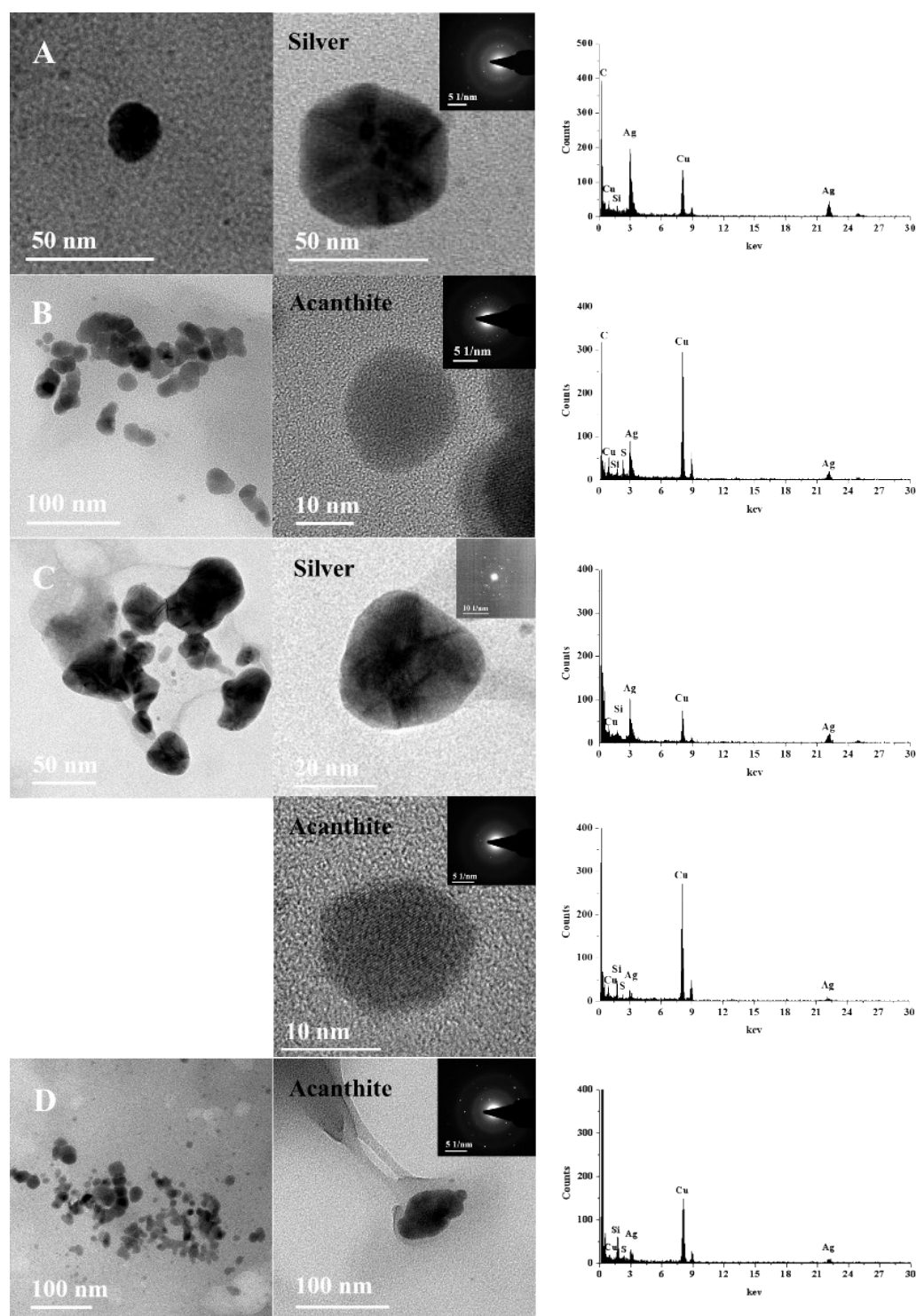


**Figure S5.** Transmission electron microscopy (TEM) analysis of Ag-NPs in *Scirpus triquetus* roots. A: Ag-NPs in plants exposed to  $\text{Ag}^+$  without SRB; B: Ag-NPs in plants exposed to  $\text{Ag}^+$  with SRB; C: Ag-NPs in plants exposed to 20-nm  $\text{Ag}^0$ -NPs without SRB; D: Ag-NPs in plants exposed to 20-nm  $\text{Ag}^0$ -NPs with SRB.

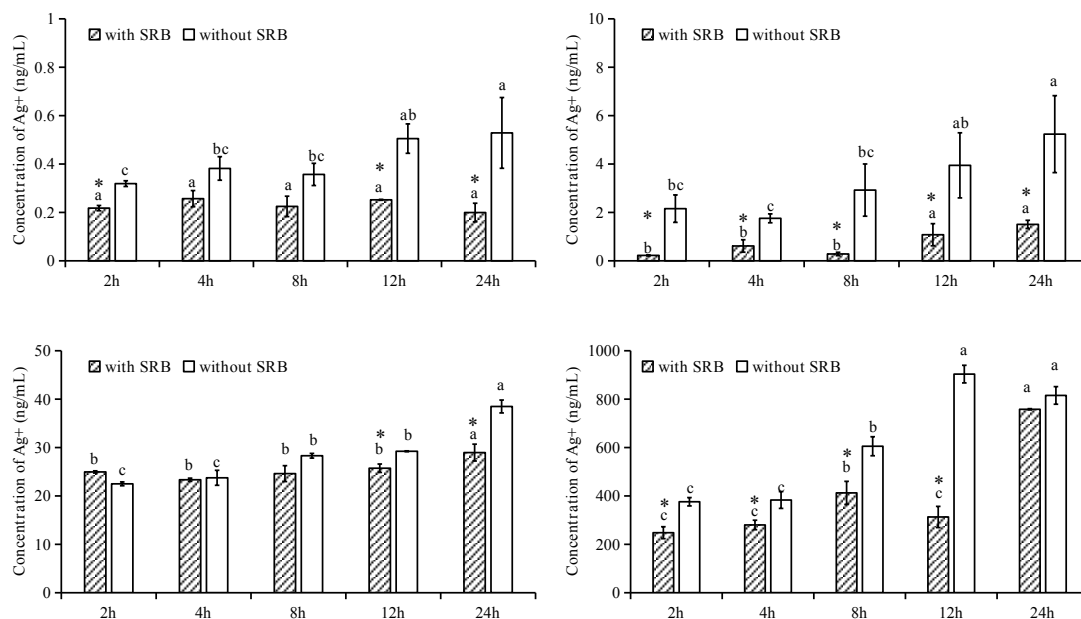


**Figure S6.** Time-dependent concentrations of dissolved Ag in 20-nm Ag<sup>0</sup>-NPs treated Hoagland solution (without plants). A: 0.01 mg/L; B: 0.1 mg/L; C: 1 mg/L and D: 10 mg/L. \*: Significant difference between the groups treated with and without SRB,  $P < 0.05$ . Different letters above the error bars indicate statistically significant differences of Ag<sup>+</sup> concentrations at different time points for the treatment group with and without SRB, respectively. ( $P < 0.05$ ).

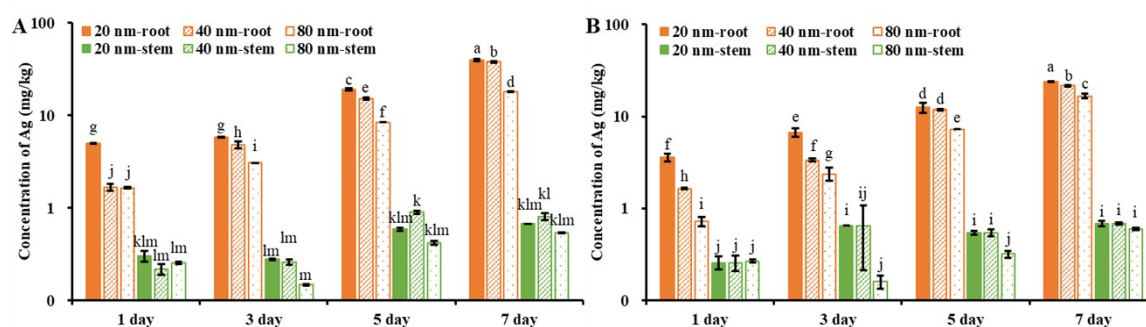


**Figure S7.** Concentrations of total Ag in *Scirpus triqueter* exposed to 0.1 mg/L 20-, 40- and 80-nm Ag<sup>0</sup>-NPs with (A) and without (B) SRB. Different letters above the error bars indicate statistically significant differences ( $P < 0.05$ ).

**Table S4.** Ratios (%) of total Ag concentrations in the whole plants treated with SRB versus those without SRB (i.e.  $R_{+/-}$ ) for 0.1 mg/L 20-, 40- and 80-nm Ag<sup>0</sup>-NPs treatment groups.

Concentration (mg/L)	Time	20-nm Ag <sup>0</sup> -NPs	40-nm Ag <sup>0</sup> -NPs	80-nm Ag <sup>0</sup> -NPs
----------------------	------	----------------------------	----------------------------	----------------------------

		treatment group	treatment group	treatment group
	1 day	138.49	213.20	100.93
	3 day	114.17	128.73	143.51
0.1	5 day	151.99	115.67	128.65
	7 day	164.32	107.49	174.97
Average		142.24	141.27	137.01
Maximum		164.32	213.20	174.97
Minimum	□	114.17	107.49	100.93

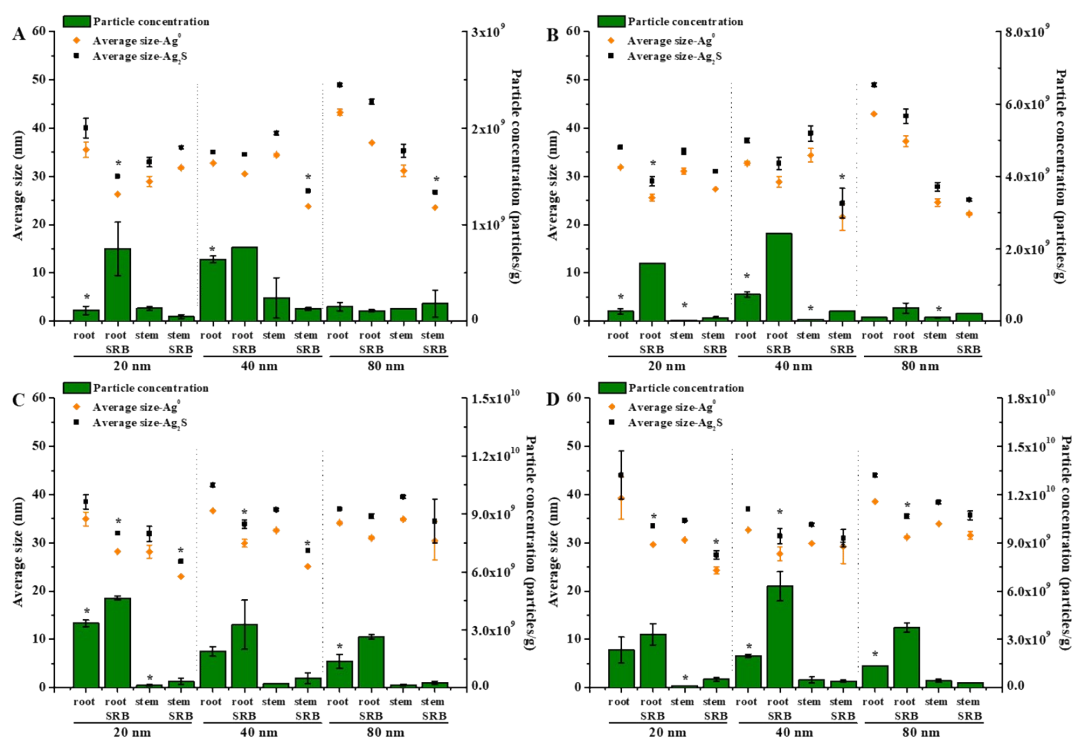


**Figure S8.** Particle concentration and size of Ag-NPs in 0.1 mg/L 20-, 40- and 80-nm Ag<sup>0</sup>-NPs treated *Scirpus triquetra* collected on the 1st day (A), 3rd day (B), 5th day (C) and 7th day (D). Root/Stem SRB: Root/Stem of *Scirpus triquetra* treated in Hoagland solution in the presence of SRB; Root/Stem: Root/Stem of *Scirpus triquetra* treated in Hoagland solution in the absence of SRB. Average size-Ag<sup>0</sup>: the average sizes were calculated based on Ag<sup>0</sup>; Average size-Ag<sub>2</sub>S: the average sizes were calculated based on Ag<sub>2</sub>S. \*: Significant difference,  $P < 0.05$ .

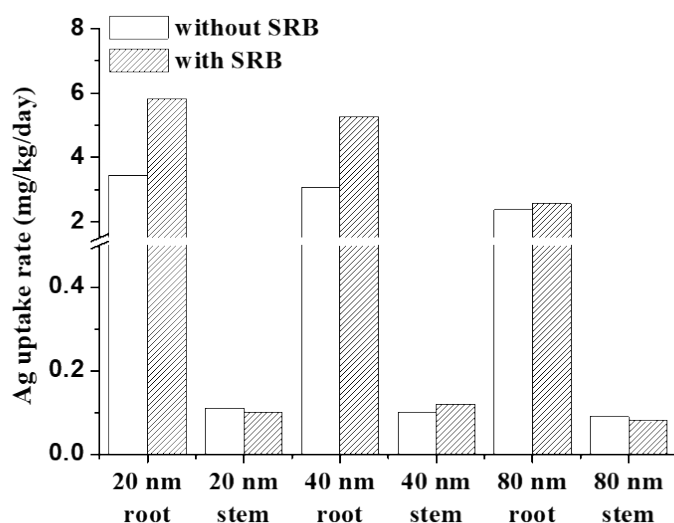


**Figure S9.** The average total Ag uptake rate (mg/kg/day) of plants exposed to 0.1 mg/L Ag<sup>0</sup>-NPs with different sizes.

## References

- 1 Y. F. Li, X. P. Guo, J. L. Yang, X. Liang, W. Y. Bao, P. J. Shen, Z. Y. Shi and J. L. Li, Effects of bacterial biofilms on settlement of plantigrades of the mussel *Mytilus coruscus*, *Aquaculture*, 2014, **433**, 434-441.
- 2 I. K. Suh, H. Ohta and Y. Waseda, High-temperature thermal expansion of six metallic elements measured by dilatation method and X-ray diffraction, *J. Mater. Sci.*, 1988, **23**, 757-760.
- 3 E. R. Jette and F. Foote, Precision determination of lattice constants, *J. Chem. Phys.*, 1935, **3**, 605-616.
- 4 A. J. Frueh, The crystallography of silver sulfide, Ag<sub>2</sub>S, *Z. Kristallogr*, 1958, **110**, 136-144.
- 5 J. P. Stegemeier, B. P. Colman, F. Schwab, M. R. Wiesner and G. V. Lowry, Uptake and distribution of silver in the aquatic plant *Landoltia punctata* (duckweed) exposed to silver and silver sulfide nanoparticles, *Environ. Sci. Technol.*, 2017, **51**, 4936-4943.
- 6 D. Hebbalalu, J. Lalley, M. N. Nadagouda and R. S. Varma, Greener techniques for the synthesis of silver nanoparticles using plant extracts, enzymes, bacteria, biodegradable polymers, and microwaves, *ACS Sustain. Chem. Eng.*, 2013, **1**, 703-712.
- 7 V. Makarov, A. Love, O. Sinitsyna, S. Makarova, I. Yaminsky, M. Taliansky and N. Kalinina, "Green" nanotechnologies: synthesis of metal nanoparticles using plants, *Acta Naturae*, 2014, **6**,

35-44.